Published in final edited form as:
Exp Cell Res. 2014 February 15; 321(2): 297–306. doi:10.1016/j.yexcr.2013.11.005.

Biomimetic scaffold combined with electrical stimulation and growth factor promotes tissue engineered cardiac development

Hyoungshin Park[1], **Benjamin L. Larson**[2], **Martin E. Kolewe**[2], **Gordana Vunjak-Novakovic**[3], and **Lisa E. Freed**[1,2,*]

[1] Biomedical Microsystems Development Group, Charles Stark Draper Laboratory, Cambridge, MA

[2] Harvard-MIT Division of Health Sciences and Technology, David H. Koch Institute for Integrative Cancer Research, and Institute of Medical Engineering and Science, MIT, Cambridge, MA

[3] Department of Biomedical Engineering, Columbia University, New York, NY

Abstract

Toward developing biologically sound models for the study of heart regeneration and disease, we cultured heart cells on a biodegradable, microfabricated poly(glycerol sebacate)(PGS) scaffold designed with micro-structural features and anisotropic mechanical properties to promote cardiac-like tissue architecture. Using this biomimetic system, we studied individual and combined effects of supplemental insulin-like growth factor-1 (IGF-1) and electrical stimulation (ES). On culture day 8, all tissue constructs could be paced and expressed the cardiac protein troponin-T. IGF-1 reduced apoptosis, promoted cell-to-cell connectivity, and lowered excitation threshold, an index of electrophysiological activity. ES promoted formation of tissue-like bundles oriented in parallel to the electrical field and a more than tenfold increase in matrix metalloprotease-2 (MMP-2) gene expression. The combination of IGF-1 and ES increased 2D projection length, an index of overall contraction strength, and enhanced expression of the gap junction protein connexin-43 and sarcomere development. This culture environment, designed to combine cardiac-like scaffold architecture and biomechanics with molecular and biophysical signals, enabled functional assembly of engineered heart muscle from dissociated cells and could serve as a template for future studies on the hierarchy of various signaling domains relative to cardiac tissue development.

Keywords

Heart; poly(glycerol sebacate); Insulin-like growth factor-1; Electrical stimulation; Anisotropy

*Corresponding author: L.E. Freed, 555 Technology Square, MS-32, Cambridge, MA 02139-4307 Lfreed@draper.com, Lfreed@mit.edu, Telephone: 617-258-4234, Fax: 617-258-3858.

Disclosure: The Authors have no competing financial interests.

Introduction

Cardiovascular disease is the leading cause of death in the United States and other developed countries. Cardiac tissue engineering aims to create a graft of viable, contractile tissue that can integrate with damaged heart tissue and enhance its contractile function [1]. Native heart muscle is a highly cellular, vascularized, compliant tissue made of aligned, differentiated, synchronously contractile cells [2, 3]. To recapitulate some of these properties, a mixed population of neonatal rat heart cells was seeded on a microfabricated elastomeric scaffold, supplemented with IGF-1 to enable cell viability and spreading, and stimulated with a pulsatile electric field to guide the assembly of a contractile tissue. As the scaffold material, we selected PGS developed by Wang et al. [4] and recently reviewed [5, 6]. We previously showed that PGS is amenable to fabrication into scaffolds with precisely controllable micro-structural features by laser drilling [7–9], laser microablation [10, 11], and silicon wafer micromolding [12–15]. Moreover, PGS mechanical properties can be tuned to mimic those of native myocardium [10, 16]. As a result, PGS scaffolds have been shown to support the *in vitro* formation of synchronously contractile cardiac constructs [7, 9–11, 13, 14, 17] with demonstrated cardiac repair potential *in vivo* [17–20]. However, progress in the field remains limited by the insufficient survival, differentiation and contractile function of engineered cardiac tissue. The aim of the present work was to test an *in vitro* environment designed to mimic specific aspects of the *in vivo* cardiac milieu with respect to an appropriate cell culture substrate combined with biological and biophysical signaling.

The design of our PGS scaffold was based on the ultimate goals of using a biodegradable biomaterial to both provide mechanical support and deliver cells to help repair a damaged heart [21]. Previous studies showed that cardiomimetic mechanical properties of microfabricated PGS scaffolds could be achieved by optimizing polymer curing conditions and exploiting intentionally designed pore patterns to impart directionally dependent resistance to strain (anisotropy) [10, 13]. In the present study, the scaffold pores (~241 μm long, ~113 μm wide, ~142 μm deep), struts (~61 μm wide) and pore pattern (cubic rectangular) were selected because we previously showed this scaffold design enabled cell-to-cell interconnectivity and contractile response to electrical stimulation; an underlying PGS membrane (~6 μm thick) was included to improve heart cell seeding efficiency [13].

Supplemental IGF-1 (100 ng/mL) was added because it is known to have beneficial effects on cardiac cells and tissue [22–25] and the viability, differentiation, contractile amplitude, and excitation threshold of engineered cardiac constructs *in vitro* [26, 27]. Biophysical signals intrinsic to native heart muscle function were provided by electrical stimulation (ES) (monophasic square pulses, 2 ms duration, 5 V/cm amplitude, 1 Hz frequency), which are known to enhance the assembly of contractile cardiac constructs *in vitro* [9, 28–32]. As the combination of these two important cues and their potential synergies has not been evaluated, we hypothesized that supplemental IGF-1 could enable cell viability and spreading while applied pulsatile ES could guide cell alignment, together yielding a more functional cardiac tissue construct. We systematically interrogated the effects of IGF-1 and ES on constructs made by culturing neonatal rat heart cells on microfabricated PGS scaffolds in four experimental groups: (i) without ES/without IGF-1 (−ES−IGF), (ii) without ES/with IGF-1 (−ES+IGF), (iii) with ES/without IGF-1 (+ES−IGF), and (iv) with ES/with IGF-1 (+ES+IGF).

Materials and Methods

Materials

Glycerol, sebacic acid, phalloidin-fluorescein isothiocyanate (FITC), trypsin, lipase and maltose were from Sigma (St. Louis, MO). DRAQ5 was from Axxora LLC (San Diego, CA). Type II collagenase was from Worthington Biochemical (Lakewood, NJ). Antibodies to troponin-T (Tn-T) and connexin-43 (Cx-43) were from Abcam (Cambridge, MA). Taqman® Universal PCR Master Mix and Taqman expression systems were from Applied Biosystems (Foster City, CA). Recombinant human IGF-1 was from BD Biosciences (San Jose, CA). Terminal deoxynucleotidyl transferase biotin 2'-deoxyuridine 5'-triphosphate nick end labeling assay (TUNEL) was from R&D systems (Minneapolis, MN). Dulbecco's Modified Eagle Medium (DMEM), fetal bovine serum (FBS), penicillin/streptomycin (pen/strep), Trypsin-EDTA, Trizol, and RNA-to-Ct 1 Step Kit were from Invitrogen (Carlsbad, CA). Carbon rod electrodes and platinum wire were from Ladd Research (Williston, VT).

PGS scaffold biofabrication

Silicon wafer molds were made as previously described [13–15]. Briefly, Mylar mask transparencies generated by CAD/ART Service (Brandon, OR) were used to micropattern 4-inch diameter silicon wafers by standard photolithography and reactive ion etching. The etched wafers were prepared for use by oxygen plasma treatment (100 W for 30 s) using a Plasma Asher (PX-250, March Plasma Systems, Concord, CA) and spin-coating of a sacrificial layer of maltose, 70% (w/v), using an EE100 spinner (Brewer Science, Rolla, MO). PGS pre-polymer was synthesized by poly-condensation of glycerol and sebacic acid [4, 33], dissolved in ethanol, 25% (v/v), cast in silicon wafer molds, and vacuum cured at 165°C for 8 h at 15 mTorr [13]. Cured PGS scaffolds were delaminated from the molds by soaking in deionized water at 60°C for 2 to 3 days. Scaffolds were cut to final dimensions (7 mm long × 4 mm wide × 100 μm high), autoclave-sterilized at 121°C for 20 min, and incubated in culture medium (DMEM supplemented with 10% FBS and 1x pen/strep) at 37°C for 5 days with one medium exchange prior to cell seeding.

Cardiac construct preparation

Heart cells were obtained from 1 to 2 day old neonatal Sprague Dawley rats (n=70) as previously described [11, 13]. All animals were handled following a protocol approved by an Institutional Animal Care and Use Committee. The ventricles were serially digested in trypsin (0.6 mg/mL at 4°C for 16 h) and then Type II collagenase (1 mg/mL at 37°C). PGS scaffolds were blotted dry and placed individually in 12 well plates within poly(dimethylsiloxane) (PDMS) gaskets (10 mm long × 6 mm wide × 0.5 mm high). Freshly harvested heart cells were seeded (5 million cells in 30 μL of culture medium per scaffold), incubated for 30 minutes in a 37°C incubator, and then 3 mL of culture medium were added to each well; PDMS gaskets were gently removed after 24 h. Four experimental groups were defined as follows: (i) −ES−IGF; (ii) −ES+IGF; (iii) +ES−IGF; and (iv) +ES+IGF. One day after cell seeding, constructs were subdivided such that in groups (i) and (iii) the medium was unsupplemented, whereas in groups (ii) and (iv) the medium was supplemented with 100 ng/mL of IGF-1. Three days after cell seeding, constructs were transferred into ES dishes (four constructs and 35 mL of the appropriate culture medium per dish), and ES was initiated in groups (iii) and (iv). The ES protocol was based on previous studies [28, 30] in which we showed that applied ES promoted myocardial tissue development and that monophasic square pulses, 2 ms in duration, 5 V/cm amplitude, 1 Hz frequency started on culture day three resulted in the best histological and contractile properties of constructs based on neonatal rat heart cells and collagen sponge scaffolds. In the present study, the ES dishes were 100 mm diameter glass Petri dishes fitted with two parallel carbon rod electrodes separated by a 1 cm gap that was further subdivided by PDMS partitions into four

rectangular compartments (12 mm long × 10 mm wide). Constructs were positioned with respect to the electrodes such that the scaffold long pore direction was aligned in parallel to the electrodes. In groups (iii) and (iv), the electrodes were connected via platinum wires to an electrical pulse stimulator (S88x Dual Output Square Pulse Stimulator, Grass Technologies, West Warwick, RI). Culture medium was completely replaced every 3 days, and constructs were harvested for evaluation on day 8.

Mechanical testing

Scaffolds were mechanically tested as previously described [10, 13]. In brief, dry scaffolds were cut using a dog-bone punch (gauge length 5 mm, width 2 mm), thickness was measured using a dial gauge (L.S. Starrett Co., Athol, MA), and the samples were mounted on a mechanical tester (Electroforce ELF 3200, Bose, Framingham, MA) and strained to failure. Independent samples (at least four per group and time point) were tested in the long pore direction (PD) and short pore direction (XD), to assess anisotropy. Effective stiffness (E), ultimate tensile strength (UTS) and strain to failure (ε) data were calculated from the stress-strain data.

Microscopy

For scanning electron microscopy (SEM), dry PGS scaffolds were sputter-coated with Au-Pd alloy using a 108 Auto/SE Sputter Coater (Cressington Scientific Instruments, Watford, UK) and examined using a Hitachi S3500 SEM (Hitachi High Technologies America, Pleasanton, CA). For transmission electron microscopy (TEM), cardiac constructs were fixed in 2.5% glutaraldehyde and 3% paraformaldehyde with 5% sucrose in 0.1 M sodium cacodylate buffer (pH 7.4) and postfixed in 1% OsO_4 in veronal acetate buffer. The samples were stained, dehydrated and embedded in Spurr's resin. Sections were cut at 50 nm using a microtome (Reichert Ultracut E) with diamond knife (Diatome) and the sections were examined using an EM410 TEM instrument (Philips, Eindhoven, The Netherlands) at 80 kV. For confocal microscopy, *c*onstructs were fixed in 10% neutral buffered formalin for 24 h at 4°C, permeabilized using 0.1% Triton X-100, blocked with 0.1% bovine serum albumin, stained with either phalloidin-FITC or Tn-T, counterstained with DRAQ5 nuclear stain, and examined using a Nikon A1R-A1 confocal laser microscope (Melville, NY). For histological analyses, formalin-fixed constructs were paraffin-embedded and sectioned to 5 μm thickness, stained, and examined using a Zeiss Axiovert 200M microscope (Carl Zeiss Inc., Germany). Apoptosis was assessed by the TUNEL assay and quantified as a percentage of total cells as previously described [26], and Cx-43 was assessed after immunostaining. Collagen was assessed after staining with Masson's trichrome.

Electrophysiological testing

Excitation threshold (ET) was assessed as previously described [14,26]. In brief, constructs were transferred to a temperature-controlled ES dish, monophasic 2 ms square pulses were applied at 1 Hz, and the voltage was increased incrementally while observing contractions at 10x magnification using a Zeiss Axiovert 200M microscope. The ET was measured as the voltage at which synchronously contractile cells were observed. A 2D projection length was defined by using a modification of the procedure described by Shim et al [34]. In the same temperature-controlled ES dish, constructs were recorded at 2.5x magnification using a digital videocamera (Fire-I Unibrain Inc. San Ramon, CA). Individual frames from the videos corresponding to relaxed and maximally contracted states were processed by using a custom MATLAB program, in which a Harris corner detection algorithm was used to automatically detect corners of the scaffold. The difference in corner position between the two frames was used as the 2D projection length.

Quantitative real time polymerase chain reaction (qPCR)

Gene expression levels were quantified as previously described [11] using Taqman® Universal PCR Master Mix. Total RNA was isolated by homogenization in Trizol followed by extraction in chloroform and precipitation using a RNeasy Mini kit (Qiagen, Valencia, CA). qPCR was performed with RNA-to-Ct 1 Step Kit using two gene-specific primers: Tn-T and matrix metalloprotease-2 (MMP-2). Gene expression was normalized to glyceraldehyde 3-phosphate dehydrogenase (GAPDH) and then relative expression was calculated.

Statistical analysis

Data were analyzed by analysis of variance using Statistica version 7 (StatSoft, Tulsa, OK). Individual differences between groups were determined by Turkey's *post hoc* analysis. Statistical significance was established at $p < 0.05$.

3. Results

PGS scaffold structure, mechanical properties, and biodegradation

PGS scaffolds with rectangular wells (241 ± 2 μm long, 113 ± 0.4 μm wide, and 142 ± 5 μm deep), separated by intervening struts (61 ± 5 μm wide) and with a thin underlying PGS membrane (6 ± 2 μm thick) were consistently produced by silicon wafer replica molding (Fig. 1). Mechanical testing in two orthogonal directions confirmed anisotropy, with higher stiffness in the direction of the long pore axis than the short pore axis (E_{PD}: 589 ± 39 kPa *versus* E_{XD}: 361 ± 22 kPa, p=0.001). Likewise, ultimate tensile strength was higher in the direction of the long pore axis (UTS_{PD}: 319 ± 36 kPa v*ersus* UTS_{XD}; 195 ± 33 kPa, p=0.039); strain to failure was high and similar in both directions (ε_{PD}: 0.87 ± 0.1 ~ ε_{XD}: 0.80 ± 0.1). Rapid scaffold biodegradation *in vitro* was confirmed by incubation with lipase. Upon incubation, PGS scaffolds with dimensions of 7 mm × 4 mm biodegraded completely within 3 h in 2,000 U/mL lipase and within 5 h in 500 U/mL lipase. The structural, mechanical, and degradation data described herein are consistent with the previous studies showing that biodegradable PGS scaffolds can be fabricated at relatively high throughput with precisely controllable microstructures and anisotropic, elastomeric mechanical properties [6, 13, 14, 35].

Effects of supplemental IGF-1

Supplemental IGF-1 significantly reduced apoptosis by ANOVA ($p<0.005$) (Figs. 2B, 2D, 2I). In addition, collagenous extracellular matrix (ECM) deposition appeared more prevalent with supplemental IGF-1 (Figs. 2 F and 2H). While expression of the cardiac-specific protein Tn-T and the cytoskeletal protein F-Actin were observed in all groups (Fig. 3), supplemental IGF-1 without ES enhanced spatially uniform cell-to-cell interconnectivity throughout the PGS scaffold in group (ii) (Figs. 3D and 3E). Supplemental IGF-1 reduced ET in group (ii) as compared to group (i) (p=0.001) with an interactive effect of IGF-1 and ES in group (iv) (p=0.013) (Fig. 4). Immunohistochemical and electrophysiological data described herein suggest that supplemental IGF-1 reduced apoptosis, promoted heart cell spreading and reduced ET, thereby enabling the formation of a functionally contractile syncytium.

Effects of ES

The presence of ES, with or without IGF-1, was associated with the formation of tissue-like bundles oriented in parallel to the direction of the electric field in group (iii) (Fig. 3G) and group (iv) (Fig. 3J). ES increased MMP-2 gene expression by more than ten-fold with an individual effect of ES (p=0.0002) and an interactive effect of ES and IGF-1 (p=0.0003)

(Fig. 5B). Morphological and gene expression data presented herein suggest that ES promoted ECM remodeling in cardiac constructs, directing tissue-like bundle formation and increasing MMP-2 gene expression.

Combined effects of supplemental IGF-1 and ES

Immunostaining showed Cx-43 protein was clearly abundant when IGF-1 and ES were both present (Fig. 6D), less prevalent if either one or the other factor was absent (Figs. 6B and 6C), and minimal if both factors were absent (Fig. 6A). Likewise, sarcomeres were best developed when IGF-1 and ES were both present (Fig. 7D), somewhat developed when one or the other factor was absent (Figs. 7B and 7C), and disorganized if both factors were absent (Fig. 7A). Moreover, IGF-1 and ES individually and interactively affected 2D projection length, an index of cardiac contractility (IGF-1, p=0.0002; ES, p=0.0002; IGF-1 and ES, p=0.0002) (Fig. 8). Immunohistochemical, ultrastructural, and videoimaging data described herein suggest interactive effects of supplemental IGF-1 and ES on gap junction formation, sarcomere development, and an index of contractile activity.

4. Discussion

The novelty of the current work is in its integrated approach, wherein architectural, molecular and electrophysiological elements are combined to guide the assembly of engineered heart tissue. Native development of the heart – the first functional organ in the human body, which starts to beat and pump blood three weeks into gestation – involves sequences of molecular and biophysical factors. After cell commitment and specification during early stages of development, further steps include factors involved in physiological hypertrophy (such as IGF-1) and electromechanical coupling (electrical stimulation) [36–39]. At all stages, the combination of factors and the timing of their application determine functional cell and tissue outcomes. Here, we probed for interactive effects by culturing heart cells in a microenvironment combining *(i)* a poly(glycerol sebacate)(PGS) scaffold with structural and mechanical properties matching some aspects of native cardiac tissue, *(ii)* a molecular factor, IGF-1, and (*iii*) a physical factor, ES. We showed the assembly of engineered heart tissue was enabled by these three factors, acting individually and in concert, and presumably recapitulating some aspects of the *in vivo* developmental milieu. We believe that such an integrated approach can help advance our limited understanding of the complex roles of scaffold design features [13], insulin-related factors [40], and electrical signals [41] on cardiac development and function, with implications to tissue engineering and regenerative medicine.

The structure and mechanical properties of our PGS scaffold were based on the ultimate goals of using a biodegradable biomaterial to both deliver cells and provide mechanical support to help repair a damaged heart [21]. To enable high cell density, we selected scaffolds with deep (~142 μm) rectangular (~241 μm long, 113 μm wide) pores separated from each other by thin (~61 μm wide) struts and bounded below by a very thin, underlying PGS membrane (~6 μm thick). This design enabled scaffold seeding with high cell density while maintaining anisotropy and high strain to failure. Scaffold stiffness was increased by two-fold as compared to similar scaffolds without underlying membranes [13], and was approximately five times higher than that previously measured for left ventricular myocardium [11]. With respect to biological function, the selected scaffold design enabled cell-to-cell interconnectivity and the *in vitro* development of a functional syncytium, as assessed by two structural measures (immunohistochemistry and TEM) and two measures of contractility (ET and 2D projection length).

We focused on exploring additional effects of a molecular cue (IGF-1) and a biophysical cue (ES) in the context of heart cells cultured on our cardiomimetic PGS scaffold. IGF-1 is

known to be important for cell growth and viability, and the mechanisms underlying these effects are known to involve the IGF-1 receptor (IGF-1R), the MEK-ERK signaling pathway for cell growth and proliferation, and the PI3K-Akt signaling pathways for muscle hypertrophy and preventing cardiomyocyte apoptosis [42–45]. Moreover, ES is known to stabilize action potential [46], increase peak calcium current [39] and enhance calcium transient [47]

The present study showed that, when used individually, either IGF-1 or ES could improve heart cell viability, promote formation of muscle tissue-like bundles, increase MMP-2 gene expression, and lower excitation threshold. These findings were consistent with previous studies that involved either IGF-1 [26, 27] or ES [28, 30] individually. However, in contrast to previously used collagen sponge scaffolds, we selected PGS, a mechanically robust synthetic elastomer [4, 5] that can be reproducibly microengineered into scaffolds with precise, cardiomimetic microarchitectures [10, 13, 14].

Moreover, the present study was the first demonstration of interactive effects of ES and IGF-1, factors that were not previously tested in combination, on heart muscle development in the context of engineered cardiac tissue. The interactive effects of ES and IGF-1 included higher expression of Cx-43 protein, well developed sarcomeres, and increased 2D projection length, an index of contractility. As compared to the excitation threshold, used as an indicator of electrophysiological function, the 2D projection length is intended to be a measure of overall contraction strength [48]. To successfully generate heart muscle contractions, the cells must be healthy at both the molecular and functional levels. Based on collected data, the interactive effects of IGF-I and ES may be explained by (i) IGF-1 enabling heart cell physiology by promoting anti-apoptotic activity, cardiac myocyte differentiation and cardiac fibroblast proliferation, and (ii) ES enabling heart cell functionality by inducing assembly of contractile proteins and gap junctions.

As a further extension of the present study, incorporation of electroactive polymers that can sense, conduct and/or deliver electrical stimuli would be an interesting approach. Several electroactive polymers have been explored with cultured cells, including myoblasts, such as conductive polyaniline [49], polypyrrole-co-polycaprolactone [50], nanostructured conductive platforms comprised of aligned multi-walled carbon nanotubes and polypyrrole [51], and free-standing nanowire nanoelectronic scaffolds [52]. In addition, controlled local release of small bioactive molecules like IGF-1 via scaffold modification may improve their efficacy [53].

Conclusions

The *in vitro* development of heart cells into contractile tissue was enabled in a microenvironment that combined (*i*) a microfabricated scaffold with structural and mechanical properties matching some aspects of native heart muscle, (*ii*) a molecular factor, IGF-1, and (*iii*) a biophysical factor, ES, to recapitulate some aspects of the *in vivo* cardiac developmental milieu. In this context, IGF-1 and ES individually and interactively enabled cell viability, cell spreading, extracellular matrix deposition, expression of the gap junction protein connexin 43, contractility, and sarcomere development. The integrated approach presented here can help advance our limited understanding of the complex and interconnected roles of structural support, electrical signaling, and molecular cues on cardiac development and function, with implications to the creation of functional tissue for regenerative medicine.

Acknowledgments

This work was funded by the National Heart, Lung and Blood Institute (NHLBI) (award 1-R01-HL107503 to LEF, and Cancer Center Support Grant CA014051 to the Koch Center for Integrative Cancer Research). The content is solely the responsibility of the authors and does not necessarily represent the official views of the NHLBI or NIH. We thank James Hsaio, Ernest Kim and Patrick Wu for help with silicon micromolding and PGS scaffold preparation, and Eliza Vasile and Nicki Watson for help with microscopy.

References

[1]. Vunjak-Novakovic G, Tandon N, Godier A, Maidhof R, Marsano A, Martens TP, et al. Challenges in cardiac tissue engineering. Tissue Eng Part B Rev. 2010; 16:169–87. [PubMed: 19698068]

[2]. Fijnvandraat AC, Lekanne Deprez RH, Moorman AF. Development of heart muscle-cell diversity: a help or a hindrance for phenotyping embryonic stem cell derived cardiomyocytes. Cardiovasc Res. 2003; 58:303–12. [PubMed: 12757865]

[3]. Mercola M, Ruiz-Lozano P, Schneider MD. Cardiac muscle regeneration: lessons from development. Genes Dev. 2011; 25:299–309. [PubMed: 21325131]

[4]. Wang Y, Ameer GA, Sheppard BJ, Langer R. A tough biodegradable elastomer. Nat Biotechnol. 2002; 20:602–6. [PubMed: 12042865]

[5]. Rai R, Tallawi M, Grigore A, Boccaccini AR. Synthesis, properties and biomedical applications of poly(glycerol sebacate) (PGS): A review. Progress in Polymer Science. 2012; 37:1051–78.

[6]. Chen Q, Liang S, Thouas GA. Elastomeric biomaterials for tissue engineering. Progress in Polymer Science. 2013; 38:584–671.

[7]. Radisic M, Park H, Chen F, Salazar-Lazzaro JE, Wang Y, Dennis RG, et al. Biomimetic approach to cardiac tissue engineering: Oxygen carriers and channeled scaffolds. Tissue Eng. 2006; 12:2077–91. [PubMed: 16968150]

[8]. Maidhof R, Marsano A, Lee EJ, Vunjak-Novakovic G. Perfusion seeding of channeled elastomeric scaffolds with myocytes and endothelial cells for cardiac tissue engineering. Biotechnol Prog. 2010; 26:565–72. [PubMed: 20052737]

[9]. Maidhof R, Tandon N, Lee EJ, Luo J, Duan Y, Yeager K, et al. Biomimetic perfusion and electrical stimulation applied in concert improved the assembly of engineered cardiac tissue. J Tissue Eng Regen Med. 2012; 6:e12–23. [PubMed: 22170772]

[10]. Engelmayr GC Jr. Cheng M, Bettinger CJ, Borenstein JT, Langer R, Freed LE. Accordion-like honeycombs for tissue engineering of cardiac anisotropy. Nat Mater. 2008; 7:1003–10. [PubMed: 18978786]

[11]. Park H, Larson BL, Guillemette MD, Jain SR, Hua C, Engelmayr GC Jr. et al. The significance of pore microarchitecture in a multi-layered elastomeric scaffold for contractile cardiac muscle constructs. Biomaterials. 2011; 32:1856–64. [PubMed: 21144580]

[12]. Guillemette MD, Park H, Hsiao JC, Jain SR, Larson BL, Langer R, et al. Combined technologies for microfabricating elastomeric cardiac tissue engineering scaffolds. Macromol Biosci. 2010; 10:1330–7. [PubMed: 20718054]

[13]. Neal RA, Jean A, Park H, Wu PB, Hsiao J, Engelmayr GC Jr. et al. Three-dimensional elastomeric scaffolds designed with cardiac-mimetic structural and mechanical features. Tissue Eng Part A. 2013; 19:793–807. [PubMed: 23190320]

[14]. Kolewe ME, Park H, Gray C, Ye X, Langer R, Freed LE. 3D structural patterns in scalable elastomeric polymer scaffolds guide engineered tissue architecture. Adv Mater. 2013; 25:4459–65. [PubMed: 23765688]

[15]. Ye X, Lu L, Kolewe ME, Park H, Larson BL, Kim ES, et al. Biodegradable microvessel scaffold as a framework to enable vascular support of engineered tissues. Biomaterials. 2013; 34:10007–15. [PubMed: 24079890]

[16]. Chen QZ, Bismarck A, Hansen U, Junaid S, Tran MQ, Harding SE, et al. Characterisation of a soft elastomer poly(glycerol sebacate) designed to match the mechanical properties of myocardial tissue. Biomaterials. 2008; 29:47–57. [PubMed: 17915309]

[17]. Radisic M, Park H, Martens TP, Salazar-Lazaro JE, Geng W, Wang Y, et al. Pre-treatment of synthetic elastomeric scaffolds by cardiac fibroblasts improves engineered heart tissue. J Biomed Mater Res A. 2008; 86:713–24. [PubMed: 18041719]

[18]. Chen QZ, Ishii H, Thouas GA, Lyon AR, Wright JS, Blaker JJ, et al. An elastomeric patch derived from poly(glycerol sebacate) for delivery of embryonic stem cells to the heart. Biomaterials. 2010; 31:3885–93. [PubMed: 20153041]

[19]. Stuckey DJ, Ishii H, Chen QZ, Boccaccini AR, Hansen U, Carr CA, et al. Magnetic resonance imaging evaluation of remodeling by cardiac elastomeric tissue scaffold biomaterials in a rat model of myocardial infarction. Tissue Eng Part A. 2010; 16:3395–402. [PubMed: 20528670]

[20]. Marsano A, Maidhof R, Luo J, Fujikara K, Konofagou EE, Banfi A, et al. The effect of controlled expression of VEGF by transduced myoblasts in a cardiac patch on vascularization in a mouse model of myocardial infarction. Biomaterials. 2013; 34:393–401. [PubMed: 23083931]

[21]. Freed LE, Engelmayr GC Jr. Borenstein JT, Moutos FT, Guilak F. Advanced material strategies for tissue engineering scaffolds. Adv Mater. 2009; 21:3410–8. [PubMed: 20882506]

[22]. Davis ME, Hsieh PC, Takahashi T, Song Q, Zhang S, Kamm RD, et al. Local myocardial insulin-like growth factor 1 (IGF-1) delivery with biotinylated peptide nanofibers improves cell therapy for myocardial infarction. Proc Natl Acad Sci USA. 2006; 103:8155–60. [PubMed: 16698918]

[23]. Suleiman MS, Singh RJ, Stewart CE. Apoptosis and the cardiac action of insulin like growth factor I. Pharmacol Ther. 2007; 114:278–94. [PubMed: 17499363]

[24]. Jiang S, Haider HK, Idris NM, Ashraf M. Abstract 1416: IGF-1 gene transfer promotes connexin-43 expression and enhances integration of bone marrow stem cells in the infarcted heart. Circulation. 2008; 118:S_321.

[25]. Ruvinov E, Leor J, Cohen S. The promotion of myocardial repair by the sequential delivery of IGF-1 and HGF from an injectable alginate biomaterial in a model of acute myocardial infarction. Biomaterials. 2011; 32:565–78. [PubMed: 20889201]

[26]. Cheng MY, Park H, Engelmayr GC, Moretti M, Freed LE. Effects of regulatory factors on engineered cardiac tissue in vitro. Tissue Eng. 2007; 13:2709–19. [PubMed: 17708718]

[27]. Cheng M, Moretti M, Engelmayr GC, Freed LE. Insulin-like growth factor-I and slow, bi-directional perfusion enhance the formation of tissue-engineered cardiac grafts. Tissue Eng Part A. 2009; 15:645–53. [PubMed: 18759675]

[28]. Radisic M, Park H, Shing H, Consi T, Schoen FJ, Langer R, et al. Functional assembly of engineered myocardium by electrical stimulation of cardiac myocytes cultured on scaffolds. Proc Natl Acad Sci USA. 2004; 101:18129–34. [PubMed: 15604141]

[29]. Tandon N, Marsano A, Cannizzaro C, Voldman J, Vunjak-Novakovic G. Design of electrical stimulation bioreactors for cardiac tissue engineering. Conf Proc IEEE Eng Med Biol Soc. 2008; 2008:3594–7. [PubMed: 19163486]

[30]. Tandon N, Cannizzaro C, Chao PH, Maidhof R, Marsano A, Au HT, et al. Electrical stimulation systems for cardiac tissue engineering. Nat Protoc. 2009; 4:155–73. [PubMed: 19180087]

[31]. Barash Y, Dvir T, Tandeitnik P, Ruvinov E, Guterman H, Cohen S. Electric field stimulation integrated into perfusion bioreactor for cardiac tissue engineering. Tissue Eng Part C Methods. 2010; 16:1417–26. [PubMed: 20367291]

[32]. Chiu LL, Iyer RK, King JP, Radisic M. Biphasic electrical field stimulation aids in tissue engineering of multicell-type cardiac organoids. Tissue Eng Part A. 2011; 17:1465–77. [PubMed: 18783322]

[33]. Neeley WL, Redenti S, Klassen H, Tao S, Desai T, Young MJ, et al. A microfabricated scaffold for retinal progenitor cell grafting. Biomaterials. 2008; 29:418–26. [PubMed: 17961646]

[34]. Shim J, Grosberg A, Nawroth JC, Parker KK, Bertoldi K. Modeling of cardiac muscle thin films: pre-stretch, passive and active behavior. J Biomech. 2012; 45:832–41. [PubMed: 22236531]

[35]. Pomerantseva I, Krebs N, Hart A, Neville CM, Huang AY, Sundback CA. Degradation behavior of poly(glycerol sebacate). J Biomed Mater Res A. 2009; 91:1038–47. [PubMed: 19107788]

[36]. Chien KR, Knowlton KU, Chien S. Regulation of cardiac gene expression during myocardial growth and hypertrophy: molecular studies of an adpative physiology response. FASEB J. 1991; 5:3037–46. [PubMed: 1835945]

[37]. Nuccitelli R. Endogenous ionic currents and DC electric fields in multicellular animal tissues. Bioelectromagnetics. 1992; (Suppl 1):147–57. [PubMed: 1285710]

[38]. Zhao M, Forrester JV, McGaig CD. A small, physiological electric field orients cell division. Proc Natl Acad USA. 1999; 96:4942–6.

[39]. Berger HJ, Prasad SK, Davidoff AJ, Pimental D, Ellingsen O, Marsh JD, et al. Continual electric field stimulation preserves contractile function of adult ventricular myocytes in primary culture. Am J Physiol. 1994; 266:H341–H9. [PubMed: 8304516]

[40]. Lian X, Zhang J, Zhu K, Kamp TJ, Palecek SP. Insulin inhibits cardiac mesoderm, not mesendoderm, formation during cardiac differentiation of human pluripotent stem cells and modulation of canonical Wnt signaling can rescue this inhibition. Stem Cells. 2013; 31:447–57. [PubMed: 23193013]

[41]. Tandon N, Marsano A, Maidhof R, Wan L, Park H, Vunjak Novakovic G. Optimization of electrical stimulation parameters for cardiac tissue engineering. J Tissue Eng Regen Med. 2011; 5:e115–25. [PubMed: 21604379]

[42]. Buerke M, Murohara T, Skurk C, Nuss C, Tomaselli K, Lefer AM. Cardioprotective effect of insulin-like growth factor I in myocardial ischemia followed by reperfusion. Proc Natl Acad Sci USA. 1995; 92:8031–5. [PubMed: 7644533]

[43]. Coolican SA, Samuel DS, Ewton DZ, McWasde FJ, Florini JR. The mitogenic and myogenic actions of insulin-like growth factors utilize distinct signaling pathways. J Biol Chem. 1997; 272:6653–62. [PubMed: 9045696]

[44]. Rommel C, Bodine SC, Clarke BA, Rossman R, Nunez L, Stitt TN, et al. Mediation of IGF-1 induced skeletal myotube hypertrophy by PI(3)K/Akt/mTOR and PI(3)K/Akt/GSK3 pathways. Nat Cell Biol. 2001; 3:1009–13. [PubMed: 11715022]

[45]. Laustsen PG, Russell SJ, Cui L, Entingh-Pearsall A, Holzenberger M, Liao R, et al. Essential role of insulin and insulin-like growth factor 1 receptor signaling in cardiac development and function. Mol Cell Biol. 2007; 27:1649–64. [PubMed: 17189427]

[46]. Sathaye A, Bursac N, Tung L. Electrical pacing counteracts intrinsic shortening of action potential duration of neonatal rat ventricular cells in culture. J Mol Cell Cardiol. 2006; 41:633–41. [PubMed: 16950369]

[47]. Holt E, Lunde PK, Sejersted OM, Christensen G. Electrical stimulation of adult rat cardiomyocytes in culture improves contractile properties and is associated with altered calcium handling. Basic Res Cardiol. 1997; 92:289–98. [PubMed: 9486350]

[48]. Feinberg AW, Alford PW, Jin H, Ripplinger CM, Werdich AA, Sheehy SP, et al. Controlling the contractile strength of engineered cardiac muscle by hierarchal tissue architecture. Biomaterials. 2012; 33:5732–41. [PubMed: 22594976]

[49]. Bidez PR, Li S, Macdiarmid AG, Venancio EC, Wei Y, Lelkes PI. Polyaniline, an electroactive polymer, supports adhesion and proliferation of cardiac myoblasts. J Biomater Sci Polym Ed. 2006; 17:199–212. [PubMed: 16411609]

[50]. Nguyen HT, Sapp S, Wei C, Chow JK, Nguyen A, Coursen J, et al. Electric field stimulation through a biodegradable polypyrrole-co-polycaprolactone substrate enhances neural cell growth. J Biomed Mater Res A. 2013 doi: 10.1002/jbm.a.34925. [Epub ahead of print].

[51]. Quigley AF, Razal JM, Kita M, Jalili R, Gelmi A, Penington A, et al. Electrical stimulation of myoblast proliferation and differentiation on aligned nanostructured conductive polymer platforms. Adv Healthc Mater. 2012; 1:801–8. [PubMed: 23184836]

[52]. Tian B, Liu J, Dvir T, Jin L, Tsui JH, Qing Q, et al. Macroporous nanowire nanoelectronic scaffolds for synthetic tissues. Nat Mater. 2012; 11:986–94. [PubMed: 22922448]

[53]. Nelson DM, Baraniak PR, Ma Z, Guan J, Mason NS, Wagner WR. Controlled release of IGF-1 and HGF from a biodegradable polyurethane scaffold. Pharm Res. 2011; 28:1282–93. [PubMed: 21347565]

Highlights

- Systematic studies of heart cell viability and function on a biomimetic scaffold
- IGF-1 and electrical stimulation (ES) enable gap junction and sarcomere development
- IGF-1 and ES interactively reduce excitation threshold and improve contractility

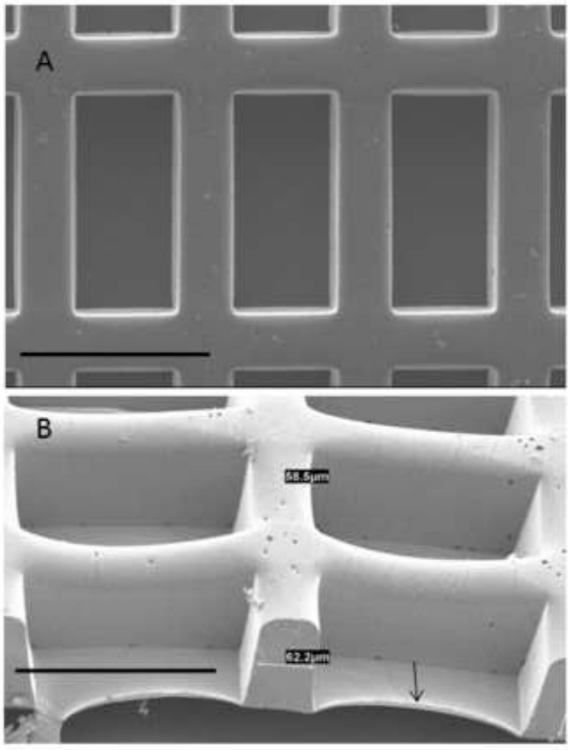

Figure 1.
Scaffold design. Scanning electron micrographs are shown in (A) top view and (B) tilt view. Arrow points to the underlying PGS membrane. Scale bars: 200 μm.

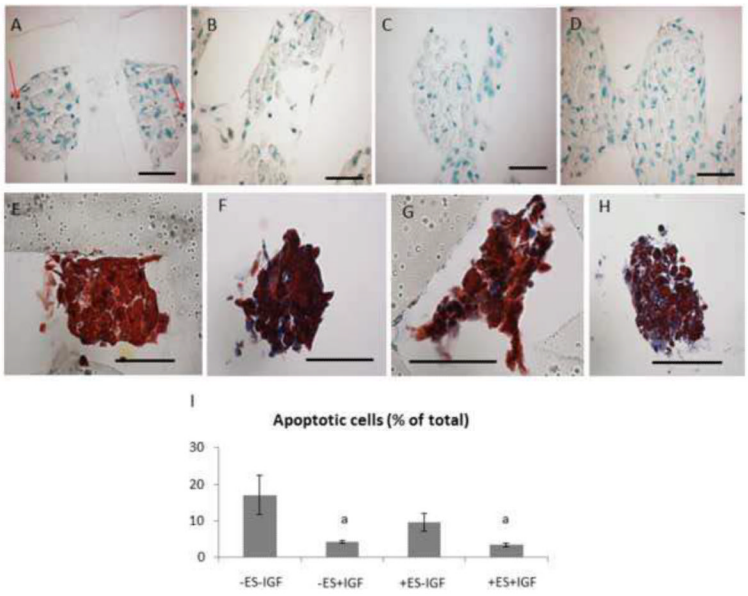

Figure 2.

Apoptosis and collagenous ECM deposition in 8-day constructs from (A,E) group (i), (B,F) group (ii), (C,G) group (iii), and (D,H) group (iv). (A–D) TUNEL stain (red arrows (A) point to apoptotic nuclei; the PGS scaffold appears translucent due to processing artifact); (E–H) Masson's trichrome stain (collagen indicated by blue color); (I) Quantification of apoptotic cells. Scale bars: 50 μm. Data are the mean ± SE of 3 to 5 specimens. (a) Significant effect of IGF ($p<0.005$).

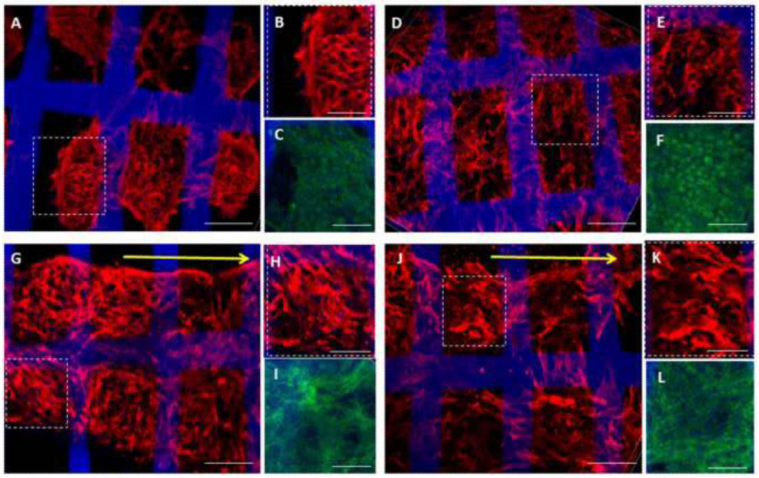

Figure 3.

Protein expression and tissue morphologies for (A–C) group (i), (D–F) group (ii), (G–I) group (iii), and (J–L) group (iv). Confocal images of 8-day constructs showed expression of the cardiac-specific marker Tn-T (A, B, D, E, G, H, J, K) and the cytoskeletal marker F-Actin (C, F, I, L) in all four groups. ES was associated with the formation of tissue-like bundles oriented in parallel to the direction of the electric field in groups (iii and iv) (G,J). Yellow arrows point in the direction of the electrical field. Tn-T: red; F-actin: green; PGS scaffold: blue. Regions of interest (dashed boxes) within full-stack confocal renderings (A, D, G, J) are also shown at higher magnification as partial stack (10-layer) confocal renderings (B, E, H, K). Scale bars: (A, D, G, J) 100 μm; (B, C, E, F, H, I, K, L) 50 μm.

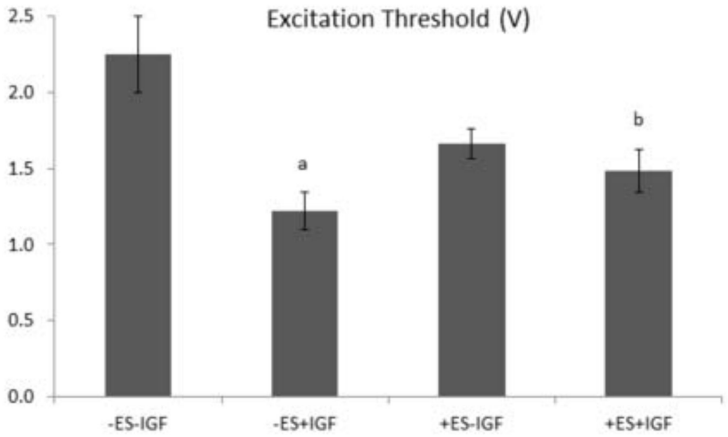

Figure 4.

Excitation threshold of 8-day constructs. Data are the mean ± SE of at least four samples. (a) Individual effect of IGF (p=0.001). (b) Interactive effect of ES and IGF (p=0.013).

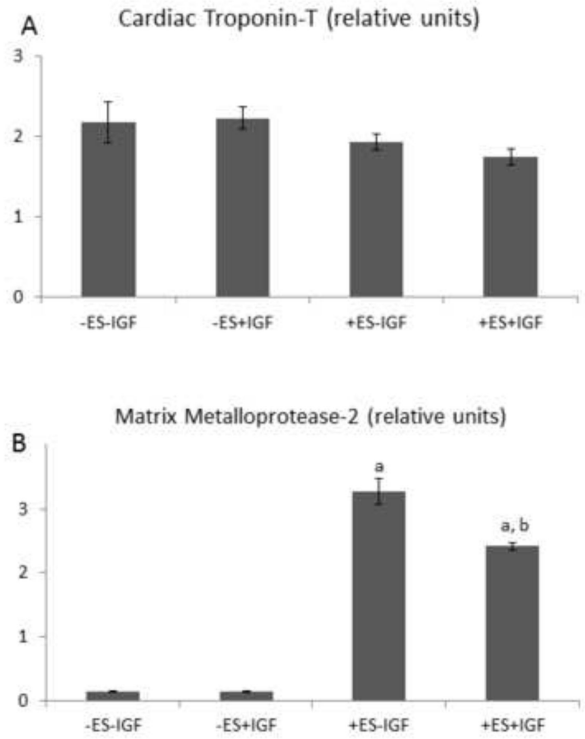

Figure 5.
Gene expression by quantitative PCR of 8 day constructs. (A) Cardiac Tn-T, (B) MMP-2. Data are the mean ± SE of six samples. (a) Individual effect of ES (p=0.0002); (b) Interactive effect of ES and IGF (p=0.0002).

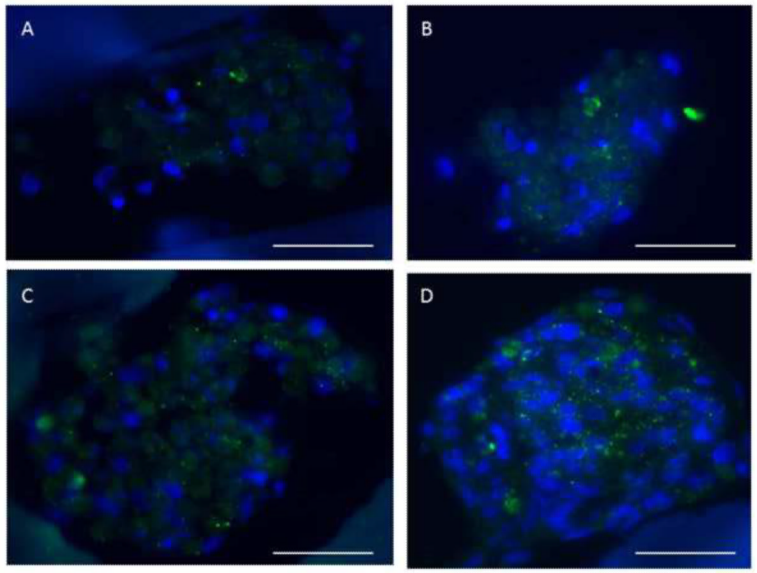

Figure 6.
Connexin-43 immunohistochemistry for 8-day constructs from (A) group (i), (B) group (ii), (C) group (iii), and (D) group (iv). The gap junction protein Cx-43 was readily observed in the presence of both IGF-1 and ES (D), less prevalent with either ES or IGF-1 alone (B,C), and minimally present without either factor (A). Cx-43: green; nuclei and PGS scaffold: blue. Scale bars: 50 μm.

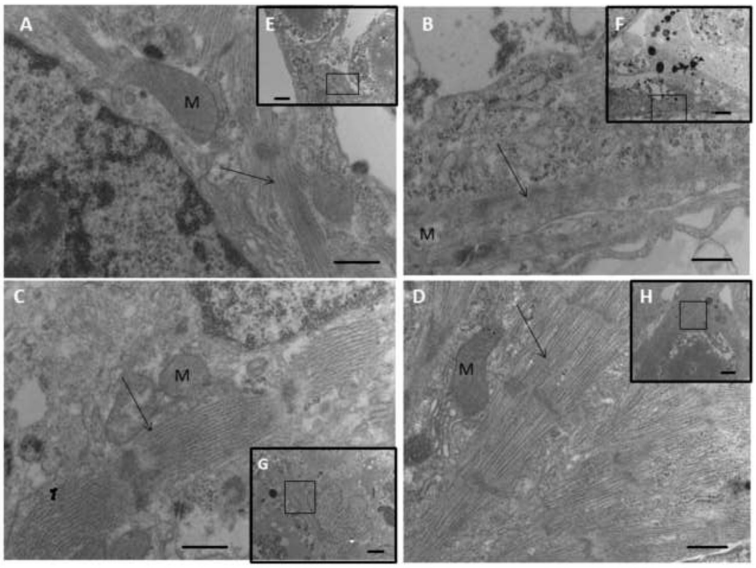

Figure 7.

Transmission electron micrographs for 8-day constructs from (A,E) group (i), (B,F) group (ii), (C,G) group (iii), and (D,H) group (iv). Sarcomeres were most developed in the presence of both IGF-1 and ES (D), less developed with either factor alone, (B,C) and relatively disorganized without either factor (A). The high magnification views shown in (A–D) are the regions of interest indicated by black squares in the low magnification insets (E–H). Arrows point to sarcomeres; M indicates mitochondrion. Scale bars: (A–D) 500 nm; (E–H) 2 μm.

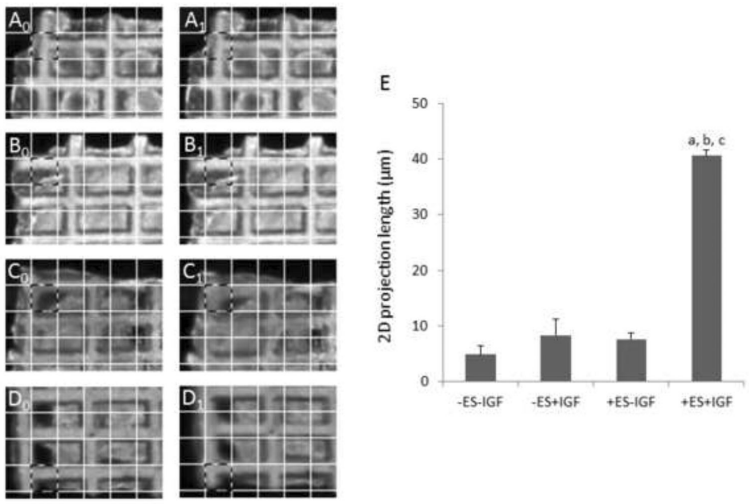

Figure 8.

2D projection length. Representative images of relaxed and contracted constructs used to calculate 2D projection lengths for (A_0,A_1) group (i), (B_0,B_1) group (ii), (C_0,C_1) group (iii), and (D_0,D_1) group (iv). Corresponding regions of interest for relaxed (X_0) and contracted (X_1) constructs (*e.g.*, A_0 and A_1, respectively) are outlined in a dashed pattern, where each grid square shown has dimensions of 120 m × 120 μm. Calculations were made from these images using an automated image processing algorithm, but qualitative differences can be noted by eye using grid squares as a reference. (E) Summary of 2D projection lengths for 8-day constructs, where data are the mean ± SE of at least 6 samples, and (a) indicates individual effect of IGF (p=0.0002), (b) indicates interactive effect of ES and IGF (p=0.0002), and (c) indicates individual effect of ES (p=0.0002).